Published in final edited form as:
Radiat Res. 2013 June ; 179(6): 617–629. doi:10.1667/RR3279.1.

Exacerbation of Lung Radiation Injury by Viral Infection: The Role of Clara Cells and Clara Cell Secretory Protein

Casey M. Manning[a], **Carl J. Johnston**[a,b], **Eric Hernady**[d], **Jennie H. Miller**[d], **Christina K. Reed**[b], **B. Paige Lawrence**[a,c], **Jacqueline P. Williams**[d], and **Jacob N. Finkelstein**[a,b,d]

[a]Department of Environmental Medicine, University of Rochester Medical Center, Rochester, New York

[b]Department of Pediatrics, University of Rochester Medical Center, Rochester, New York

[c]Department of Microbiology and Immunology, University of Rochester Medical Center, Rochester, New York

[d]Department of Radiation Oncology, University of Rochester Medical Center, Rochester, New York

Abstract

Viral infections have been associated with exacerbation of disease in human cases of idiopathic pulmonary fibrosis. Since pulmonary fibrosis is a common outcome after irradiation to the lung, we hypothesized that viral infection after radiation exposure would exacerbate radiation-induced lung injury. Epithelial injury, a frequent outcome after infection, has been hypothesized to contribute to the pathogenesis of pulmonary fibrosis and bronchiolar epithelial Clara cells participate in epithelial repair. Therefore, it was further hypothesized that altered responses after irradiation involve the bronchiolar epithelial Clara cells. C57BL/6J or $CCSP^{-/-}$ mice were irradiated with 0 (sham), 5, 10 or 15 Gy to the whole thorax. At ten weeks post-irradiation, animals were mock infected or infected with influenza A virus and body weight and survival were monitored. Pulmonary function was assessed by whole-body plethysmography. The Clara cell markers, CCSP and Cyp2f2, were measured in the lung by qRT-PCR, and protein expression was visualized in the lung by immunofluorescence. Following pulmonary function tests, mice were sacrificed and tissues were collected for pathological analysis. In 15 Gy irradiated animals infected with influenza A virus, accelerated respiratory rates, reduced pulmonary function, and exacerbated lung pathology occurred earlier post-irradiation than previously observed after irradiation alone, suggesting infection accelerates the development of radiation injury. After irradiation alone, CCSP and Cyp2f2 mRNA levels were reduced, correlating with reductions in the number of Clara cells lining the airways. When combined with infection, these markers further declined and an apparent delay in recovery of mRNA expression was observed, suggesting that radiation injury leads to a chronic reduction in the number of Clara cells that may potentiate the epithelial injury observed after influenza A virus infection. This novel finding may have considerable therapeutic implications with respect to both thoracic tumor patients and recipients of bone marrow transplants.

[1]Address for correspondence: University of Rochester School of Medicine, 601 Elmwood Ave., Box 850, Rochester, NY 14642; Jacob_Finkelstein@urmc.rochester.edu.

INTRODUCTION

Radiation-induced lung injury observed in clinical patients includes pneumonitis and fibrosis (1). The development of radiation lung injury follows a well-characterized clinical progression. After an initial period where no clinical injury can be observed, impaired lung function and lung pathology begin to develop late after radiation exposure (2). The pathogenesis of late radiation-induced lung injury remains unclear; however, an abnormal wound healing response is hypothesized to contribute to the chronic inflammation and remodeling observed after irradiation (3). Many investigators, including our own group, have suggested that critical steps in the pulmonary late effect progression involve the many molecular and cellular responses that are observed immediately after radiation exposure, including the expression of pro-inflammatory and profibrogenic cytokines, chemokines and growth factors (4–6). These factors, over time, become chronically dysregulated, causing a persistent disruption in normal pulmonary homeostasis (6–8). The resultant fibrotic changes observed in the lung after irradiation include increased extracellular matrix deposition, thickening of the lung parenchyma and restrictive pulmonary function (9). This pathology is not unlike that observed in idiopathic pulmonary fibrosis (IPF), a progressive fibrotic lung disease of unknown etiology (9). In humans with IPF, an association with herpes virus infections has been observed (10, 11), and the presence of latent, or subclinical viral infections has been hypothesized to contribute to acute exacerbations of IPF, causing rapid deterioration and high mortality (12). Indeed, animal models of pulmonary fibrosis have shown a latent viral infection can augment established fluorescein isothiocyanate (FITC)-induced pulmonary fibrosis, as well as permit bleomycin-induced fibrosis in mouse strains generally not susceptible to bleomycin (12–14).

At present, it is unknown whether viral infection exacerbates radiation-induced lung injury; however, the aforementioned studies suggest that a viral challenge in the context of a profibrotic environment can potentially result in augmented pathological responses. In support of this idea, we have previously shown that mortality levels following influenza A virus challenge are increased with prior radiation exposure (15). In this earlier study, we observed that radiation exposure followed by infection was associated with a prolonged increase in protein leakage into the lung, suggesting a possible breakdown in the pulmonary epithelium (15). Given that pulmonary epithelial cells are primarily targeted for infection by respiratory viruses such as influenza, we questioned whether prior irradiation may have disrupted normal repair of the damaged epithelium. Specifically, airway epithelial Clara cells, which are normally in a quiescent state, have the capacity to become proliferative, self-renewing and differentiating into ciliated epithelial cells to restore epithelial integrity (16). Furthermore, Clara cells are the predominant source of Clara cell secretory protein (CCSP), an anti-inflammatory mediator involved in the response to viral infections (17).

In this study, we hypothesized that viral challenge to the lung after irradiation would exacerbate radiation-induced lung injury and specifically investigated the role of the Clara cell population and CCSP in the altered response to influenza A virus challenge. C57BL/6J mice that have been irradiated with a whole-lung 15 Gy dose characteristically begin to develop radiation-induced lung pathology 26 weeks post-irradiation (18). Here, 15 Gy whole-lung irradiated C57BL/6J mice were infected with influenza A virus at 10 weeks post-irradiation to assess whether infection altered the progression of the observed radiation pathology. We similarly determined whether infection at 10 weeks after whole-lung irradiation could induce pathology in doses that are generally considered below threshold (≤10 Gy) for developing radiation injury. Lastly, we utilized a $CCSP^{-/-}$ mouse strain to determine the role of CCSP and Clara cells in the altered response to influenza A virus observed after irradiation.

MATERIALS AND METHODS

Radiation Exposure and Infection

C57BL/6J mice (female, 6–8 weeks of age) were obtained from Jackson Laboratory (Bar Harbor, ME) and were acclimated for one week prior to experimentation. $CCSP^{-/-}$ mice (female, 6–10 weeks of age) are on a C57BL/6J background and were bred in-house. Mice were housed five per cage in micro-isolator units and were supplied with standard laboratory diet and water *ad libitum*. All animal protocols were approved by the University Committee on Animal Resources at the University of Rochester.

A Cesium-137 γ-ray source operating at dose rate of approximately 2.2 Gy/min was used for all radiation exposures. For whole-lung irradiation, five unanesthetized mice per run were individually confined in plastic jigs and oriented on the collimator so that only the thoracic region was within the exposure field. Animals were exposed to the source for the time required to achieve a whole-lung dose of 5, 10 or 15 Gy. Control mice were sham-irradiated by identical handling, but were not exposed to the radiation source. At 10 weeks post-irradiation, sham and irradiated animals were intranasally infected under anesthesia (Avertin; 2,2,2-tribromoethanol; Sigma-Aldrich) with 120 Hemagglutination units (HAU) influenza virus A/ HKx31 (H3N2) in 25 μL sterile PBS. Sham and irradiated mock-infected control mice received 25 μL of sterile PBS alone. After infection, animal survival and body weight was monitored daily for 21 days in $CCSP^{-/-}$ mice, 42 days in 15 Gy whole-lung irradiated C57BL/ 6J mice, and 70 days in the 5 and 10 Gy whole-lung irradiated C57BL/ 6J mice. A set of archived tissue samples from 15 Gy whole-lung irradiated C57BL/6J mice sacrificed at 8, 12 and 26 weeks post-irradiation were also used in this study to determine lung CCSP mRNA and protein expression.

Breathing Rate Measurement

Respiratory rates were measured in unanesthetized C57BL/6J mice by whole-body plethysmography (Buxco Electronics, Inc., Wilmington, NC) on days 3, 7, 10 and 14 post-infection, then weekly afterwards up until termination of the experiment at day 42 or day 70 post-infection. A constant airflow of 1 L/min was maintained using a 4-channel bias flow regulator (Buxco Electronics, Inc.) connected to a plethysmograph. A single mouse was placed in the chamber and allowed to acclimate for approximately 3 min. Changes in airflow through the chamber were measured by a flow transducer. Data were collected and analyzed using the Biosystems XA software package (Buxco Electronics, Inc.) and respiratory rates were calculated as breaths/min from the flow data.

Pulmonary Function Measurements

Dynamic lung compliance and lung resistance were measured as previously described (19). Pulmonary function was assessed on days 14 and either days 42 or 70 post-infection in C57BL/6J mice and on days 14 and 21 post-infection in $CCSP^{-/-}$ mice. Following anesthesia, a tracheostomy was performed, and a 20-gauge cannula was inserted into an anterior nick in the exposed trachea. Each animal was placed in a plethysmograph designed for anesthetized mice (Buxco Electronics, Inc. Wilmington, NC), and connected to a Harvard rodent ventilator (Harvard Apparatus, South Natick, MA). The mouse was then ventilated with a tidal volume of 0.01 ml/g body weight at a rate of 150 breaths/min. Respiratory flow and pressure were measured using transducers attached to the plethysmograph chamber. Data were collected and analyzed using the Biosystems XA software package (Buxco Electronics). Dynamic lung compliance was calculated in ml/cm H_2O from the flow and pressure signals using the method by Amdur and Mead (20), and then normalized for peak body weight. Lung resistance values were calculated in cm H_2O/ml/s from the same input signals.

Animal Sacrifice and Sample Collection

Animals were sacrificed immediately after pulmonary function measurements. Whole blood was obtained by cardiac puncture of the left ventricle and centrifuged for plasma collection. The left lung lobe was collected and frozen in liquid nitrogen. The right lung lobe was perfused with 10 mL saline through the left ventricle of the heart and then inflation-fixed with zinc-buffered formalin. Tissue was fixed overnight, processed and embedded into paraffin blocks. Blocks were cut into 5 μm thick sections and stained with CAT Hematoxylin and Reuben's Eosin-Phloxine (H&E; Biocare Medical, Concord, CA) or Trichrome. Brightfield images were acquired at 10× magnification using a Spot Pursuit Camera (Diagnostic Instruments, Inc., Sterling Heights, MI). A separate set of $CCSP^{-/-}$ mice were sacrificed on days 9, 14 and 21 post-infection for bronchoalveolar lavage fluid collection. After perfusion, a 20-gauge catheter was inserted into an anterior nick in the trachea and secured with suture. BAL was performed using two 0.8 mL washes with buffer (1× Dulbecco's PBS, 1% glucose, 0.2 m*M* EGTA, 0.05 mg/mL Gentamicin). Cells were separated from lavage fluid by centrifugation at 1,200 rpm at 4°C for 6 min.

Immunostaining

Immunostaining was performed on formalin-fixed, paraffin-embedded lung tissue. Paraffin sections (5 μm thick) were deparaffinized and then rehydrated through graded washes of ethanols. Heat-mediated antigen retrieval was performed in Citrate buffer (10 m*M* Citric Acid, 0.05% Tween 20, pH 6.0). For CCSP immunofluorescence, slides were blocked with TBS containing 3% normal donkey serum (Vector Labs, Burlingame, CA) for 1 h at room temperature, followed by the addition of the primary antibody, goat anti-CCSP (1:2000; a gift from Barry Stripp, Duke University, Durham, NC), and incubation overnight at 4°C. Slides were washed, and incubated in secondary antibody, DyLight 594-conjugated donkey anti-goat IgG (1:200; Jackson ImmunoResearch Laboratories, Inc., West Grove, PA) for 1 h at room temperature. Nuclear counterstaining was performed with DAPI (Invitrogen, Grand Island, NY) and slides were mounted with Vectashield hardset fluorescent mounting media (Vector Labs). To detect CCSP immunohistochemically, slides were first treated with Peroxidazed 1 (Biocare Medical) to block endogenous peroxidases and blocked with Rodent Block M (Biocare Medical) for 30 min. Slides were then incubated in primary antibody, rabbit anti-CCSP (1:2000; Abcam, Cambridge, UK) for 20 min at room temperature. After washing, Rabbit-on-Rodent-HRP Polymer (Biocare Medical) was applied for 25 min at room temperature. Color was developed by reaction with Betazoid DAB Chromagen (Biocare Medical). Slides were counterstained with CAT Hematoxylin, dehydrated through graded ethanol and xylene washes, and cover slipped.

Fluorescent images were acquired at 10× magnification on a Nikon Eclipse TE2000E microscope using MetaVue Software (Molecular Devices, LLC, Sunnyvale, CA). Ten airways per animal and 3 animals per group were analyzed using Image Pro software (Media Cybernetics, Silver Spring, MD). The length of airway containing positive staining and total length of airway was calculated. Percentage positive staining was then calculated from these values.

Protein and Real-Time Polymerase Chain Reaction

Total protein in bronchoalveolar lavage fluid collected from $CCSP^{-/-}$ mice was determined using the Coomassie Plus assay (Thermo Scientific, Hanover Park, IL), according to manufacturer's instruction.

Total RNA was isolated from one half of the left lung using TRIzol reagent (Invitrogen) according to the manufacturer's instruction. One-milligram of RNA was reverse transcribed to cDNA using the Superscript III First-Strand Synthesis System (Invitrogen). Real-time

polymerase chain reaction (PCR) for CCSP and GAPDH was performed on an iCycler MyiQ2 (Bio-Rad) with the following primer sequences. CCSP: CCACAAGAGACCAGGATA (upper) and GTGAGATGCTCGCAGTTT(lower). GAPDH: CCCAATGTGTCCGTCGTG (upper) and CCTGCTTCAC CACCTTCTTG (lower). CCSP gene expression was normalized to GAPDH expression. Cyp2f2 gene expression was determined using the Taqman gene expression assay (Applied Biosystems) according to manufacturer's recommended protocol.

Statistical Analysis

Data are expressed as mean ± SEM. Statistical analyses were performed in Statview (SAS Institute Inc., Cary, NC). Group means were compared by two-way analysis of variance with the factors of radiation and infection. When a significant main effect or interaction effect was found, a Fisher's post-test was performed for paired comparisons. Survival was evaluated using Kaplan Meier plots and analyzed for significant differences using the log rank test. Differences were considered significant when $P < 0.05$.

RESULTS

Virus-Induced Exacerbation of Radiation Lung Injury

C57BL/6J mice irradiated with a whole-lung 15 Gy dose characteristically begin to develop radiation-induced lung pathology 26 weeks post-irradiation (18). To assess whether infection may adversely affect this progression, infected animals were monitored for an extended period of time (6 weeks) to allow recovery from the acute influenza challenge and were then assessed for lung structure and pulmonary function changes associated with fibrosis. After infection with influenza A virus, an approximate 30% reduction in body weight is observed by day 7 post-infection, followed by recovery of weight by day 21 post-infection. By 42 days post-infection, the surviving irradiated animals continued to have a significantly lower body weight compared to infected sham animals (Fig. 1A), which had demonstrated a complete recovery to control levels. Furthermore, mortality in the irradiation + infection group was substantial and continued to occur over time. In contrast, infected sham animals exhibited a lower mortality rate that only occurred during the peak infection period (<21 days post-infection) (Fig. 1B).

To assess progressive pulmonary function changes, respiratory rates were measured weekly, and lung compliance and resistance were measured prior to sacrifice on days 14 and 42 post-infection. Fifteen Gy irradiated animals infected with influenza A virus began to develop accelerated respiratory rates at day 28 post-infection and rates remained elevated until the end of the experiment (Fig. 2A). This increase in respiratory rate was significant compared to rates in both the infected sham- and mock-infected irradiated control groups. At day 14 post-infection, a slight reduction in lung compliance was observed in the infected groups compared to mock-infected groups, but no differences in lung compliance were found between infected sham and irradiated animals. However, at day 42 post-infection, the surviving infected, irradiated animals showed a dramatic twofold reduction in dynamic lung compliance, which was significantly different compared to both infected sham- and mock-infected irradiated groups (Fig. 2B). Similarly, lung resistance measured on day 14 post-infection in the infected groups was elevated over mock-infected controls but no difference between sham and irradiated mice was observed. By day 42 post-infection, the infected, irradiated animals showed a significant increase in lung resistance compared to both infected sham- and mock-infected irradiated groups (Fig. 2C). Histological staining was performed [Hematoxylin and Eosin (H&E) and Trichrome] to assess whether lung pathology associated with pulmonary fibrosis was present. Consistent with the observed physiological changes, H&E staining identified the presence of inflammatory cells, including foamy macrophages,

and edema within the tissue of irradiated animals at day 42 post-infection (Fig. 2D). Increased collagen deposition and thickening of the alveolar septum were also observed in Trichrome stained sections (Fig. 2E). This pathology was not observed in mock-infected irradiated animals or infected sham animals.

Since 15 Gy is above the threshold for lung late effect induction in the C57BL/6J mouse strain, we wanted to investigate what effect influenza A virus infection may have on animals irradiated with doses considered below the threshold for radiation injury. Consequently, animals irradiated with 5 or 10 Gy to the lung were infected with influenza A virus at 10 weeks post-irradiation and monitored for 70 days. We have previously shown 10 Gy whole-lung irradiated animals had increased mortality compared to sham animals within the first 21 days post-infection, although the surviving animals regained the body weight lost during infection (15). After 21 days post-infection, no further deaths were observed in 5 or 10 Gy irradiated animals (data not shown). Also, no differences were observed in respiratory rates between groups throughout 70 days post-infection (data not shown). A reduction in lung compliance (Fig. 3A) and an increase in resistance (Fig. 3B) were observed in all infected groups at day 14 post-infection. At day 70 post-infection, no significant reduction in lung compliance was observed in the infected 10 Gy irradiated animals compared to sham animals (Fig. 3A). Interestingly, in the 10 Gy irradiated animals, histologic examination identified focal fibrotic lesions in the lung, including increased collagen staining and inflammation (Fig. 3C).

Radiation Reduces CCSP and CCSP-Expressing Cells

After infection, epithelial damage caused by the virus must be repaired for complete restoration of lung structure and pulmonary function to occur. CCSP was used as a marker of bronchiolar epithelial Clara cells to identify changes in this airway epithelial cell population after infection. Challenge with influenza A virus in sham-irradiated animals caused a reduction in CCSP mRNA abundance, observed at day 9 post-infection, which had returned to uninfected control levels by day 21 post-infection (Fig. 4A). Irradiated animals demonstrated a more exaggerated reduction in CCSP expression after infection, with CCSP abundance continuing to be significantly reduced on days 14 and 21 post-infection compared to the infected sham (Fig. 4A). Interestingly, mock-infected irradiated animals also displayed a significant reduction in CCSP expression compared to mock-infected sham animals (Fig. 4A). To determine if this decrease in CCSP mRNA was a result of Clara cell loss, we performed immunofluorescent staining for CCSP protein, which localizes to the secretory bodies within Clara cells. Irradiated animals demonstrated reduced CCSP staining of airway cells in both the mock-infected group and at day 14 post-infection compared to sham animals (Fig. 4B).

This reduction in CCSP observed in the mock-treated irradiated animals prompted a separate investigation into the effect of radiation alone on this cell population over time. CCSP mRNA abundance and CCSP immunohistochemistry was performed on archived tissue samples collected at 8, 12 and 26 weeks after 15 Gy whole-lung irradiation of C57BL/ 6J mice. Consistent with the observation in the influenza experiment, a reduction in CCSP mRNA abundance was observed at 12 weeks post-whole-lung irradiation (Fig. 5A). Furthermore, this reduction was more pronounced at 26 weeks post-irradiation (Fig. 5A), a time considered to be the beginning of the fibrotic phase in this animal model. The number of airway epithelial cells staining positive for CCSP also appeared to be visually reduced over time in the irradiated animals (Fig. 5B).

The Role of CCSP in the Altered Response to Influenza

To determine if a reduction in CCSP message contributes to the altered response observed after influenza, the effect of influenza on the irradiation response was evaluated in CCSP knockout (−/−) mice. It was hypothesized that if a reduction in CCSP contributed to the altered response, complete abolition of the protein would exacerbate the outcome. $CCSP^{-/-}$ mice were subjected to sham or 15 Gy whole-lung irradiation and mock-infected or infected with influenza A virus at 10 weeks post-irradiation. Body weight and survival were measured for 21 days post-infection to assess host resistance in these animals. Irradiated $CCSP^{-/-}$ mice showed significantly lower body weight at day 14 post-infection (Fig. 6A). Improvement in body weight was delayed in irradiated $CCSP^{-/-}$ mice, which occurred after day 14 post-infection, compared to sham treated $CCSP^{-/-}$ mice, which regained body weight after day 8 post-infection (Fig. 6A). Furthermore, in contrast to sham treated animals, which fully recovered body weight, irradiated $CCSP^{-/-}$ mice continued to exhibit lower body weight at day 21 post-infection (Fig. 6A). Irradiated $CCSP^{-/-}$ mice also demonstrated greater mortality after infection compared to the sham group (Fig. 6B). This pattern in body weight is consistent with what was observed in wild-type animals subjected to influenza A virus at 10 weeks post-irradiation (15). Indeed, survival after infection in irradiated $CCSP^{-/-}$ mice was comparable to irradiated wild-type, although greater mortality was observed in infected sham $CCSP^{-/-}$ mice compared to infected sham wild-type within 21 days. Because CCSP has been associated with modulating the inflammatory response to virus, we also addressed whether knocking out CCSP would alter the immune response to influenza observed after irradiation in wild-type animals. No differences were observed in virus-specific $CD8^+$ T cells and IgG antibody production between sham and irradiated $CCSP^{-/-}$ animals (data not shown).

Dynamic lung compliance and lung resistance was assessed in sham and irradiated $CCSP^{-/-}$ mice at 14 and 21 days post-infection. To compare these data to pulmonary function measurements in wild-type mice, data originally presented in Fig. 2 was re-graphed to include data from the $CCSP^{-/-}$ strain. At day 14 post-infection, there was a reduction in lung compliance in irradiated $CCSP^{-/-}$ animals compared to sham $CCSP^{-/-}$ animals (Fig. 7A). A larger reduction in compliance was observed in irradiated $CCSP^{-/-}$ mice compared to irradiated wild-type mice (Fig. 7A; $P = 0.06$). Lung resistance at day 14 was significantly increased in irradiated $CCSP^{-/-}$ animals compared to sham $CCSP^{-/-}$ mice. Irradiated $CCSP^{-/-}$ mice also demonstrated a greater increase in resistance compared to irradiated wild-type mice (Fig. 7B). Furthermore, impairment in pulmonary function remained present at day 21 post-infection in irradiated $CCSP^{-/-}$ mice compared to sham $CCSP^{-/-}$. These data show earlier and greater decline in pulmonary function following infection, suggesting CCSP loss may play a role in the early responses to infection.

Total protein in the bronchoalveolar lavage (BAL) fluid was measured to assess epithelial damage after infection. Irradiated $CCSP^{-/-}$ mice had increased BAL protein compared to sham-irradiated $CCSP^{-/-}$ mice at day 9 post-infection (Fig. 8). The elevated BAL protein levels persisted in irradiated $CCSP^{-/-}$ mice at day 14 post-infection, whereas sham-irradiated $CCSP^{-/-}$ animals demonstrated restored levels at this time point (Fig. 8). Persistent elevation in BAL protein following irradiation in $CCSP^{-/-}$ mice is similar to observations reported following infection in irradiated wild-type animals (15).

Cytochrome P450 2F2 (Cyp2f2) was used as a Clara cell marker in $CCSP^{-/-}$ mice (21) to determine whether loss of CCSP was associated with cell loss rather than protein alone. Lung Cyp2f2 mRNA in $CCSP^{-/-}$ and wild-type mice was measured on days 9, 14 and 21 post-infection by real-time PCR. Interestingly, baseline Cyp2f2 expression levels in $CCSP^{-/-}$ mice were approximately twofold greater than in wild-type and, consistent with the earlier data, prior irradiation led to a 50% reduction in Cyp2f2 expression in both strains

(Fig. 9A). Viral infection caused a significant reduction in Cyp2f2 expression at day 9 post-infection in all groups. Furthermore, significant decreases in expression were observed in the irradiated groups of both strains on day 14 post-infection and in CCSP$^{-/-}$ mice only on day 21 post-infection. This mRNA expression pattern of Cyp2f2 was consistent with that observed for CCSP in wild-type mice (Fig. 3).

Cyp2f2 immunofluorescence was performed on tissue sections of CCSP$^{-/-}$ mice to determine if the reduction in CCSP mRNA was associated with a loss of Clara cells after irradiation. Consistent with mRNA abundance, Cyp2f2 protein, identified by positive fluorescent staining, was reduced in irradiated animals compared to sham irradiated and mock-infected, at both 14 and 21 days post-infection (Fig. 9B), suggesting that, indeed, there is a loss of Cyp2f2-expressing cells along the airways in CCSP$^{-/-}$ mice after irradiation consistent with the reduced numbers of CCSP-expressing cells along the airways seen in wild-type animals (Fig. 3). Immunofluorescence for acetylated alpha-tubulin (green) was also performed on the same tissue sections to identify ciliated epithelial cells, another prominent cell type lining the airway epithelium. Positive acetylated alpha-tubulin staining was observed along the airways where Cyp2f2 staining was absent, and was more prominent in irradiated animals (Fig. 9B).

DISCUSSION

Pulmonary fibrosis is one of the most common pneumopathies caused by radiation exposure (22), but, as with many radiation-induced late effects, the underlying mechanisms of its etiology are unclear. Many investigators have drawn parallels between the pathology and progression of radiation-induced pulmonary fibrosis and idiopathic pulmonary fibrosis (IPF), a disease in which the cause is unknown. In the case of IPF, an association between virus infections and exacerbation of disease has been observed (10, 11, 14). Indeed, virus-induced exacerbation of disease has been observed in several animal models of pulmonary fibrosis, including bleomycin-induced and FITC-induced fibrosis (12, 13). Since pulmonary complications, such as fibrosis, account for significant morbidity and mortality in patients receiving radiotherapy for thoracic tumors (1), as well as in bone marrow transplant patients when irradiation is part of their conditioning regimen (23), we were interested in whether a viral challenge exacerbates the progression to radiation-induced late effects in the lung.

In this study, we used a mouse model to assess whether an influenza A virus challenge, delivered to the irradiated lung prior to the anticipated time of expression of radiation-induced fibrosis, would affect the progression to injury. We chose the mouse as a model since, similar to humans, the mouse is susceptible to developing pneumonitis and fibrosis after radiation exposure (24, 25). However, mouse strains vary in their sensitivity to radiation, and some strains appear more prone to developing alveolitis/pneumonitis whereas others develop fibrosis (24–29). We chose the C57BL/6J mouse strain because this strain is predominantly susceptible to the development of pulmonary fibrosis after radiation exposure. We are aware of recent work that has demonstrated the susceptibility of this strain to pleural effusions, an outcome not generally observed in humans after irradiation (27). However, the C57BL/6J strain demonstrates a long latent period prior to fibrosis development so that at 10 weeks post-irradiation, when viral challenge occurred, no overt injury was present in the lung. Furthermore, the time points selected for use in the current study occur before pleural effusions are generally observed in this strain (27) and, indeed, no pleural effusions were observed at any time point.

The widespread use of C57BL/6J mice means that the pathology of the radiation-induced lung late effects are well characterized in this strain (26, 30–32). In conjunction with pathological changes, the irradiated animals exhibit reduced pulmonary function (33).

Interestingly, in this study, 15 Gy irradiated animals infected with influenza A virus at 10 weeks post-irradiation developed reduced pulmonary function and accelerated respiratory rates beginning at 6 and 4 weeks post-infection, respectively. At this time, it is 16 and 14 weeks post-irradiation, much sooner than the ≥26 weeks that would normally be anticipated after irradiation alone. Reduced lung compliance and increased lung resistance were also observed in the infected 15 Gy irradiated animals at these relatively early time points, suggesting the onset of lung pathology. Indeed, increased collagen staining, indicating reduced lung elasticity, was observed in the lungs, together with inflammation and edema, which may have contributed to the increased resistance observed in these animals. These alterations therefore suggest that the infection accelerated the development of lung late effect following 15 Gy. However, we also evaluated the effect of infection in ≤10 Gy whole-lung irradiated animals, considered below the threshold for the development of radiation-induced lung injury (24). At 20 weeks post-irradiation, the relatively low dose irradiated animals infected with influenza also demonstrated a trend toward reduced pulmonary compliance, as well as presenting with focal regions of increased collagen staining and inflammation in the lung at this time. Since 20 weeks post-irradiation is considered early for fibrosis development after radiation doses that are above the threshold for eliciting lung injury, these data demonstrate that a secondary viral challenge can not only result in overt injury at an accelerated rate after doses sufficient to cause delayed lung injury, but also potentially induce lung pathology after doses below the threshold. This is consistent with our hypothesis that subclinical injury resides in the lung after exposure and can be revealed following a secondary pulmonary challenge.

In humans and animal models of pulmonary fibrosis, virus-induced exacerbations of fibrosis are commonly observed with latent viruses, such as herpes virus (14). Both influenza A, the virus used in this study, and herpes viruses target epithelial cells (34), leading some to hypothesize that epithelial cell injury contributes to the pathogenesis of pulmonary fibrosis (35). Indeed, we have previously demonstrated elevated protein levels in the lungs of irradiated animals after viral clearance has occurred (15), indicating a persistently compromised epithelium. Furthermore, the animals' failure to regain body weight after infection and prior to sacrifice (or death) suggests that the exacerbated lung injury after infection in irradiated animals may result from an inability to completely repair the pulmonary epithelium. These observations led us to assess the role of the airway epithelium in the response to both radiation and infection.

The airway epithelium is the predominant site of influenza A virus infection. In mice, the airway epithelium consists mainly of terminally differentiated ciliated cells and secretory Clara cells. These cells demonstrate slow turnover kinetics under normal conditions, however, following epithelial injury, Clara cells can enter cell cycle to self-renew and differentiate into ciliated cells (36). To assess the effects of irradiation and infection on the airway Clara cell population, the specific cell markers, CCSP and Cyp2f2, were used. After radiation exposure alone, reductions in CCSP and Cyp2f2 mRNA correlated with reduced numbers of CCSP-expressing and Cyp2f2-expressing cells, respectively, in the airway epithelium, an indication that the mRNA reduction is likely a result of Clara cell loss. Therefore, the significant reduction in CCSP and Cyp2f2 expression observed in both sham and irradiated animals on day 9 post-influenza A virus infection is likely a result of Clara cell death, since this time correlates with peak cytolytic T cell activity in the lungs after infection (37). Interestingly, radiation exposure has been shown to cause reductions in CCSP and Cyp2f2 mRNA as early as 2 weeks after 15 Gy exposure, an observation attributed to elimination of lung stem cells undergoing proliferation during the acute radiation toxic response (38). Although, we did not look earlier than 8 weeks after irradiation, we did show significant reductions in CCSP abundance at 10–12 weeks after exposure, indicating that irradiation may induce a delayed and progressive effect on stem or progenitor cell

populations, including the Clara cell population, causing cell death over time. The resultant reduction in the number of Clara cells in the lung could potentially cause delays in epithelial repair after challenge. Assuming that the return of CCSP mRNA abundance to baseline by day 21 post-infection indicates repopulation of the Clara cells in the airway (Fig. 4), the significant reduction in mRNA expression on days 14 and 21 post-infection in the irradiated groups suggests that repopulation of this cell type is certainly delayed after irradiation. This potential delay also provides an explanation for our previous observation, in which persistent protein leakage into the airspaces was observed after influenza A infection in irradiated animals (15).

The trend towards a more exaggerated response after radiation exposure and viral challenge in the $CCSP^{-/-}$ mice suggests that the radiation-induced reduction in CCSP expression itself contributes to the altered response. However, as with all genetically engineered animals, loss of the gene may have altered the phenotype of the cells. Use of Cyp2f2 as an alternative marker to identify Clara cells in the airways of the $CCSP^{-/-}$ mice showed that CCSP and Cyp2f2 expression followed the same pattern of expression after both irradiation and infection. Furthermore, the reduced staining of Cyp2f2 in irradiated tissues from the $CCSP^{-/-}$ animals was consistent with that observed in wild-type mice using the CCSP marker, supporting the suggestion that the exacerbation of injury was due to epithelial injury and a failure to repair. However, Clara cells are not the only cell type in the bronchiolar epithelium and, indeed, the epithelial layer does appear to partially recover after irradiation and infection in the $CCSP^{-/-}$ mice, although with a greater number of the ciliated epithelial cells now staining positive for acetylated alpha-tubulin (Fig. 9).

Since Clara cells function as stem cells with respect to repair of the bronchioles, we believe that radiation affects the repair of the epithelium by reducing the number of Clara cells that can act as progenitors for the ciliated cells. However, the slow turnover kinetics of this cell type suggests that the chronic and progressive loss of $CCSP^{+}$ cells seen in Fig. 5 may not be due to direct cell death. An alternative explanation for the epithelial cell depletion could be the induction of radiation-induced accelerated senescence. There is evidence in the radiation literature showing that ionizing radiation can induce cell senescence and contribute to an accelerated aged phenotype (39–41). In particular, senescence of hematopoietic stem cells (HSC) cause defective self renewal and a decrease in HSC reserves (42, 43). HSC senescence is a potential contributor to the phenomenon of early immunosenescence, often observed in irradiated individuals, in which there is a reduction in the pools of naïve CD4 and CD8 T cells (44, 45). Furthermore, ionizing radiation has been shown to induce markers of cell senescence, e.g., p16, in tissues, including lung, and these markers are observed 12 weeks after exposure (46). For example, the senescence marker, p21 cip/waf, was observed to be elevated for prolonged periods of time in mesenchymal stem cells after irradiation (47), and these cells have been identified as playing a role in lung repair (48). Furthermore, CCSP mRNA reduction *per se* could imply a reduction in lung stem cells (38) since CCSP is also expressed in stem cells that reside in the pulmonary stem cell niches, including neuroepithelial bodies and broncho-alveolar duct junctions (49, 50). Interestingly, epithelial cell senescence has also been hypothesized to contribute to pulmonary fibrosis (51). Chronic depletion of Clara cells has been shown to contribute to peribronchiolar fibrosis (52), suggesting depletion of the progenitor cell pool plays a role in fibrogenesis.

It can be speculated that there is a potential link between radiation-induced epithelial senescence and the development of pulmonary radiation injury. Further studies are needed to clarify the role of radiation-induced senescence in lung stem cells and whether this contributes to the development of radiation-induced pulmonary fibrosis. These studies may have profound implications with respect to the development of pulmonary late effects that can affect both the morbidity and mortality of patients experiencing thoracic irradiation.

Acknowledgments

The authors wish to thank Amy K. Huser for editorial assistance. This research was supported by NIAID U19 AI091036-02, T32-HL066988, P30-ES001247, and T32-ES007026.

References

1. Carver JR, Shapiro CL, Ng A, Jacobs L, Schwartz C, Virgo KS, et al. American Society of Clinical Oncology clinical evidence review on the ongoing care of adult cancer survivors: cardiac and pulmonary late effects. J Clin Oncol. 2007; 25:3991–4008. [PubMed: 17577017]
2. Williams JP, Johnston CJ, Finkelstein JN. Treatment for radiation-induced pulmonary late effects: spoiled for choice or looking in the wrong direction? Curr Drug Targets. 2010; 11:1386–94. [PubMed: 20583979]
3. Graves PR, Siddiqui F, Anscher MS, Movsas B. Radiation pulmonary toxicity: from mechanisms to management. Semin Radiat Oncol. 2010; 20:201–7. [PubMed: 20685583]
4. Johnston CJ, Piedboeuf B, Rubin P, Williams JP, Baggs R, Finkelstein JN. Early and persistent alterations in the expression of interleukin-1 alpha, interleukin-1 beta and tumor necrosis factor alpha mRNA levels in fibrosis-resistant and sensitive mice after thoracic irradiation. Radiat Res. 1996; 145:762–7. [PubMed: 8643837]
5. Johnston CJ, Williams JP, Okunieff P, Finkelstein JN. Radiation-induced pulmonary fibrosis: examination of chemokine and chemokine receptor families. Radiat Res. 2002; 157:256–65. [PubMed: 11839087]
6. Rubin P, Johnston CJ, Williams JP, McDonald S, Finkelstein JN. A perpetual cascade of cytokines postirradiation leads to pulmonary fibrosis. Int J Radiat Oncol Biol Phys. 1995; 33:99–109. [PubMed: 7642437]
7. Zhao W, Robbins ME. Inflammation and chronic oxidative stress in radiation-induced late normal tissue injury: therapeutic implications. Curr Med Chem. 2009; 16:130–43. [PubMed: 19149566]
8. Thannickal VJ, Toews GB, White ES, Lynch JP 3rd, Martinez FJ. Mechanisms of pulmonary fibrosis. Annu Rev Med. 2004; 55:395–417. [PubMed: 14746528]
9. Wilson MS, Wynn TA. Pulmonary fibrosis: pathogenesis, etiology and regulation. Mucosal Immunol. 2009; 2:103–21. [PubMed: 19129758]
10. Tang YW, Johnson JE, Browning PJ, Cruz-Gervis RA, Davis A, Graham BS, et al. Herpesvirus DNA is consistently detected in lungs of patients with idiopathic pulmonary fibrosis. J Clin Microbiol. 2003; 41:2633–40. [PubMed: 12791891]
11. Stewart JP, Egan JJ, Ross AJ, Kelly BG, Lok SS, Hasleton PS, et al. The detection of Epstein-Barr virus DNA in lung tissue from patients with idiopathic pulmonary fibrosis. Am J Respir Crit Care Med. 1999; 159:1336–41. [PubMed: 10194186]
12. McMillan TR, Moore BB, Weinberg JB, Vannella KM, Fields WB, Christensen PJ, et al. Exacerbation of established pulmonary fibrosis in a murine model by gammaherpesvirus. Am J Respir Crit Care Med. 2008; 177:771–80. [PubMed: 18187693]
13. Lok SS, Haider Y, Howell D, Stewart JP, Hasleton PS, Egan JJ. Murine gammaherpes virus as a cofactor in the development of pulmonary fibrosis in bleomycin resistant mice. Eur Respir J. 2002; 20:1228–32. [PubMed: 12449178]
14. Vannella KM, Moore BB. Viruses as co-factors for the initiation or exacerbation of lung fibrosis. Fibrogenesis Tissue Repair. 2008; 1:2. [PubMed: 19014649]
15. Manning CM, Johnston CJ, Reed CK, Lawrence BP, Williams JP, Finkelstein JN. Lung irradiation increases mortality after Influenza A virus challenge occurring late after exposure. Int J Radiat Oncol Biol Phys. 2012 S0360-3016(12)03688-7.
16. Reynolds SD, Malkinson AM. Clara cell: progenitor for the bronchiolar epithelium. Int J Biochem Cell Biol. 2010; 42:1–4. [PubMed: 19747565]
17. Harrod KS, Mounday AD, Stripp BR, Whitsett JA. Clara cell secretory protein decreases lung inflammation after acute virus infection. Am J Physiol. 1998; 275:L924–30. [PubMed: 9815110]

18. Williams JP, Brown SL, Georges GE, Hauer-Jensen M, Hill RP, Huser AK, et al. Animal models for medical countermeasures to radiation exposure. Radiat Res. 2010; 173:557–78. [PubMed: 20334528]
19. Wright TW, Gigliotti F, Finkelstein JN, McBride JT, An CL, Harmsen AG. Immune-mediated inflammation directly impairs pulmonary function, contributing to the pathogenesis of Pneumocystis carinii pneumonia. J Clin Invest. 1999; 104:1307–17. [PubMed: 10545529]
20. Amdur MO, Mead J. Mechanics of respiration in unanesthetized guinea pigs. Am J Physiol. 1958; 192:364–8. [PubMed: 13508884]
21. Stripp BR, Maxson K, Mera R, Singh G. Plasticity of airway cell proliferation and gene expression after acute naphthalene injury. Am J Physiol. 1995; 269:L791–9. [PubMed: 8572241]
22. Tsoutsou PG, Koukourakis MI. Radiation pneumonitis and fibrosis: mechanisms underlying its pathogenesis and implications for future research. Int J Radiat Oncol Biol Phys. 2006; 66:1281–1293. [PubMed: 17126203]
23. Wah TM, Moss HA, Robertson RJ, Barnard DL. Pulmonary complications following bone marrow transplantation. Br J Radiol. 2003; 76:373–9. [PubMed: 12814922]
24. Sharplin J, Franko AJ. A quantitative histological study of strain-dependent differences in the effects of irradiation on mouse lung during the intermediate and late phases. Radiat Res. 1989; 119:15–31. [PubMed: 2756106]
25. Sharplin J, Franko AJ. A quantitative histological study of strain-dependent differences in the effects of irradiation on mouse lung during the early phase. Radiat Res. 1989; 119:1–14. [PubMed: 2756101]
26. Chiang CS, Liu WC, Jung SM, Chen FH, Wu CR, McBride WH, et al. Compartmental responses after thoracic irradiation of mice: strain differences. Int J Radiat Oncol Biol Phys. 2005; 62:862–871. [PubMed: 15936571]
27. Jackson IL, Vujaskovic Z, Down JD. Revisiting strain-related differences in radiation sensitivity of the mouse lung: recognizing and avoiding the confounding effects of pleural effusions. Radiat Res. 2010; 173:10–20. [PubMed: 20041755]
28. O'Brien TJ, Letuve S, Haston CK. Radiation-induced strain differences in mouse alveolar inflammatory cell apoptosis. Can J Physiol Pharmacol. 2005; 83:117–122. [PubMed: 15759058]
29. Paun A, Haston CK. Genomic and genome-wide association of susceptibility to radiation-induced fibrotic lung disease in mice. Radiother Oncol. 2012
30. Franko AJ, Sharplin J. Development of fibrosis after lung irradiation in relation to inflammation and lung function in a mouse strain prone to fibrosis. Radiat Res. 1994; 140:347–355. [PubMed: 7972687]
31. Moore BB, Hogaboam CM. Murine models of pulmonary fibrosis. Am J Physiol Lung Cell Mol Physiol. 2008; 294:L152–160. [PubMed: 17993587]
32. Johnston CJ, Williams JP, Elder A, Hernady E, Finkelstein JN. Inflammatory cell recruitment following thoracic irradiation. Exp Lung Res. 2004; 30:369–382. [PubMed: 15204829]
33. Travis EL, Down JD, Holmes SJ, Hobson B. Radiation pneumonitis and fibrosis in mouse lung assayed by respiratory frequency and histology. Radiat Res. 1980; 84:133–143. [PubMed: 7454976]
34. Thompson CI, Barclay WS, Zambon MC, Pickles RJ. Infection of human airway epithelium by human and avian strains of influenza a virus. J Virol. 2006; 80:8060–8. [PubMed: 16873262]
35. Selman M, Pardo A. Role of epithelial cells in idiopathic pulmonary fibrosis: from innocent targets to serial killers. Proc Am Thorac Soc. 2006; 3:364–72. [PubMed: 16738202]
36. Stripp BR, Reynolds SD. Maintenance and repair of the bronchiolar epithelium. Proc Am Thorac Soc. 2008; 5:328–33. [PubMed: 18403328]
37. Kohlmeier JE, Woodland DL. Immunity to respiratory viruses. Annu Rev Immunol. 2009; 27:61–82. [PubMed: 18954284]
38. Bernard ME, Kim H, Rajagopalan MS, Stone B, Salimi U, Rwigema JC, et al. Repopulation of the irradiation damaged lung with bone marrow-derived cells. In Vivo. 2012; 26:9–18. [PubMed: 22210711]
39. Sabin RJ, Anderson RM. Cellular Senescence - its role in cancer and the response to ionizing radiation. Genome Integr. 2011; 2:7. [PubMed: 21834983]

40. Richardson RB. Ionizing radiation and aging: rejuvenating an old idea. Aging (Albany NY). 2009; 1:887–902. [PubMed: 20157573]
41. Park HR, Jo SK. Lasting effects of an impairment of Th1-like immune response in gamma-irradiated mice: A resemblance between irradiated mice and aged mice. Cell Immunol. 2011; 267:1–8. [PubMed: 21092942]
42. Wang Y, Schulte BA, LaRue AC, Ogawa M, Zhou D. Total body irradiation selectively induces murine hematopoietic stem cell senescence. Blood. 2006; 107:358–66. [PubMed: 16150936]
43. Wang Y, Schulte BA, Zhou D. Hematopoietic stem cell senescence and long-term bone marrow injury. Cell Cycle. 2006; 5:35–8. [PubMed: 16319536]
44. Park HR, Jo SK, Paik SG. Factors effecting the Th2-like immune response after gamma-irradiation: low production of IL-12 heterodimer in antigen-presenting cells and small expression of the IL-12 receptor in T cells. Int J Radiat Biol. 2005; 81:221–31. [PubMed: 16019931]
45. Kusunoki Y, Hayashi T. Long-lasting alterations of the immune system by ionizing radiation exposure: implications for disease development among atomic bomb survivors. Int J Radiat Biol. 2008; 84:1–14. [PubMed: 17852558]
46. Le ON, Rodier F, Fontaine F, Coppe JP, Campisi J, DeGregori J, et al. Ionizing radiation-induced long-term expression of senescence markers in mice is independent of p53 and immune status. Aging Cell. 2010; 9:398–409. [PubMed: 20331441]
47. Mehrara BJ, Avraham T, Soares M, Fernandez JG, Yan A, Zampell JC, et al. p21cip/WAF is a key regulator of long-term radiation damage in mesenchyme-derived tissues. FASEB J. 2010; 24:4877–88. [PubMed: 20720160]
48. Mora AL, Rojas M. Aging and lung injury repair: a role for bone marrow derived mesenchymal stem cells. J Cell Biochem. 2008; 105:641–7. [PubMed: 18759327]
49. Giangreco A, Reynolds SD, Stripp BR. Terminal bronchioles harbor a unique airway stem cell population that localizes to the bronchoalveolar duct junction. Am J Pathol. 2002; 161:173–82. [PubMed: 12107102]
50. Reynolds SD, Giangreco A, Power JH, Stripp BR. Neuroepithelial bodies of pulmonary airways serve as a reservoir of progenitor cells capable of epithelial regeneration. Am J Pathol. 2000; 156:269–78. [PubMed: 10623675]
51. Chilosi M, Doglioni C, Murer B, Poletti V. Epithelial stem cell exhaustion in the pathogenesis of idiopathic pulmonary fibrosis. Sarcoidosis Vasc Diffuse Lung Dis. 2010; 27:7–18. [PubMed: 21086900]
52. Perl AK, Riethmacher D, Whitsett JA. Conditional depletion of airway progenitor cells induces peribronchiolar fibrosis. Am J Respir Crit Care Med. 2011; 183:511–21. [PubMed: 20870756]

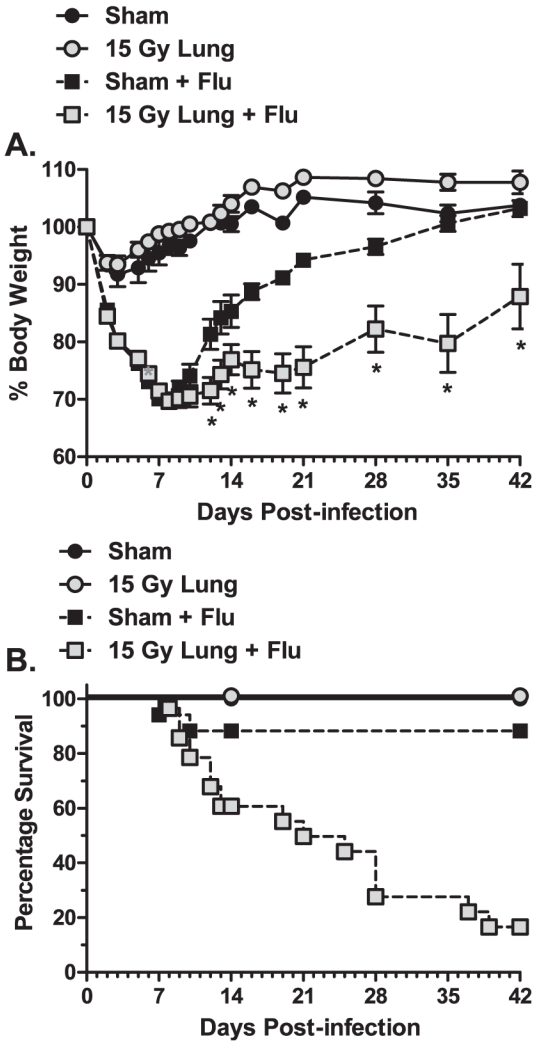

FIG. 1.

Morbidity and mortality after influenza A virus infection in sham and 15 Gy whole-lung irradiated C57BL/6J mice. At 10 weeks post-irradiation, sham and 15 Gy whole-lung irradiated mice were infected with 120 HAU influenza A virus and monitored for 42 days. Panel A: Body weight changes over time. Changes in body weight are expressed as a percentage of body weight at the time of infection. (Two-way ANOVA with Fisher's post-test, $*P < 0.05$ versus sham-infected, $n = 30$ for virus-infected groups, $n = 7$ for mock-infected groups.) Panel B: Kaplan-Meier survival curves presenting mean survival of each group over time. Curves were analyzed using the log rank test. A significant difference in mortality was observed between the sham-infected and irradiated-infected group ($P = 0.0006$).

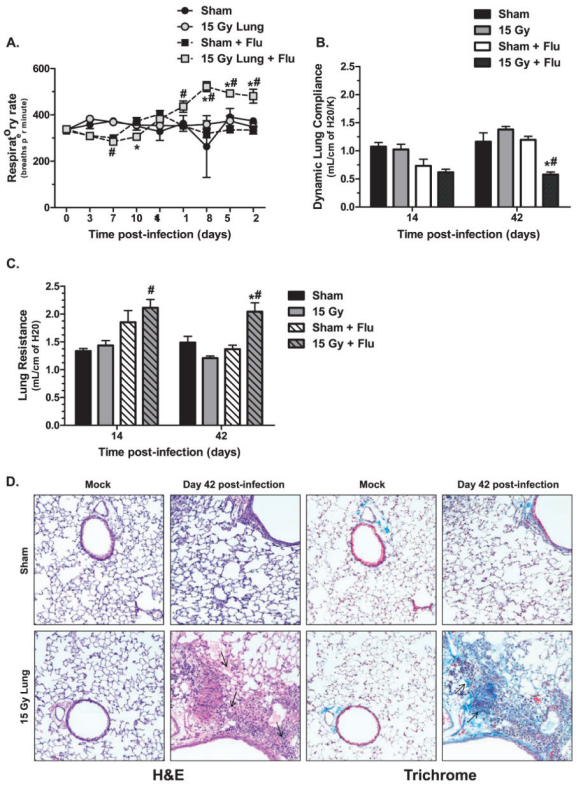

FIG. 2.

Lung function and pathology after infection in sham and 15 Gy whole-lung irradiated C57BL/6J mice. Whole-body plethysmography was used to assess pulmonary function changes after infection. Panel A: Respiratory rate over time. (*$P < 0.05$ versus mock-infected control, #$P < 0.05$ versus sham-infected, $n = 30$ for virus-infected groups, $n = 7$ for mock-infected groups.) Panel B: Dynamic lung complicance and (panel C) lung resistance at days 14 and 42 post-infection. Data are mean ± SEM of 3–6 animals per group. Data were analyzed by two-way ANOVA with Fisher's post-test. (*$P < 0.05$ versus mock-infected control, #$P < 0.05$ versus sham-infected.) Panel D: Hematoxylin and eosin staining (H&E) (left two columns) and trichrome staining (right two columns) of sham and 15 Gy irradiated lungs at day 42 post mock or influenza A virus infection. Images (20×) are representative of 3–6 mice per group.

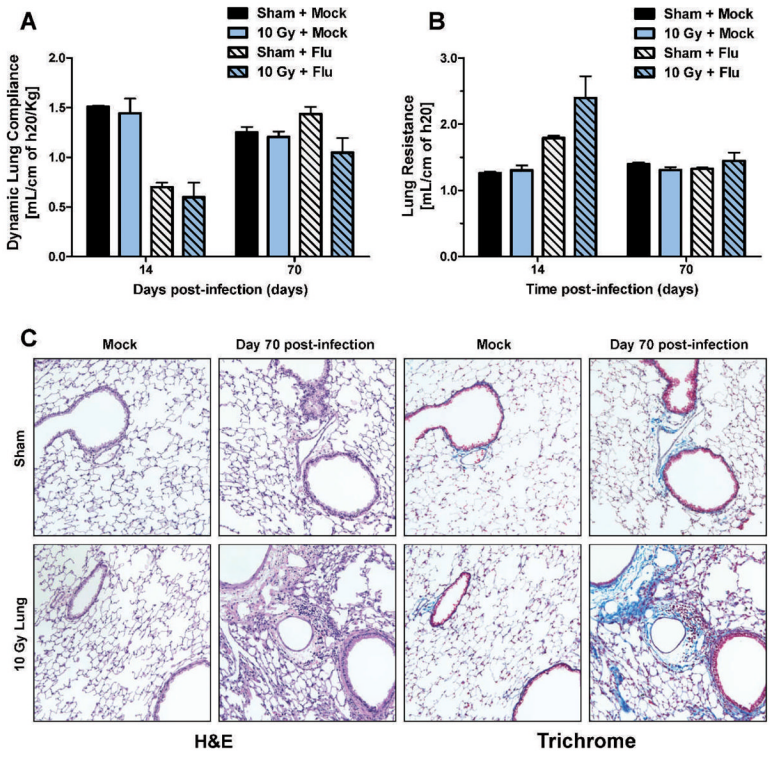

FIG. 3.

Lung function and pathology after infection in sham and 10 Gy whole-lung irradiated C57BL/6J mice. Whole-body plethysmography was used to assess pulmonary function changes after infection in animals irradiated at 10 Gy whole-lung dose. Panel A: Dynamic lung compliance and (panel B) lung resistance at days 14 and 70 post-infection. Data are mean ± SEM of 3–4 animals per group. Data were analyzed by two-way ANOVA. No significant differences were observed. Panel C: Hematoxylin and Eosin staining (H&E) (left two columns) and Trichrome staining (right two columns) of sham and 10 Gy irradiated lungs at day 70 post-mock or influenza A virus infection. Images (20×) are representative of 3–4 mice per group.

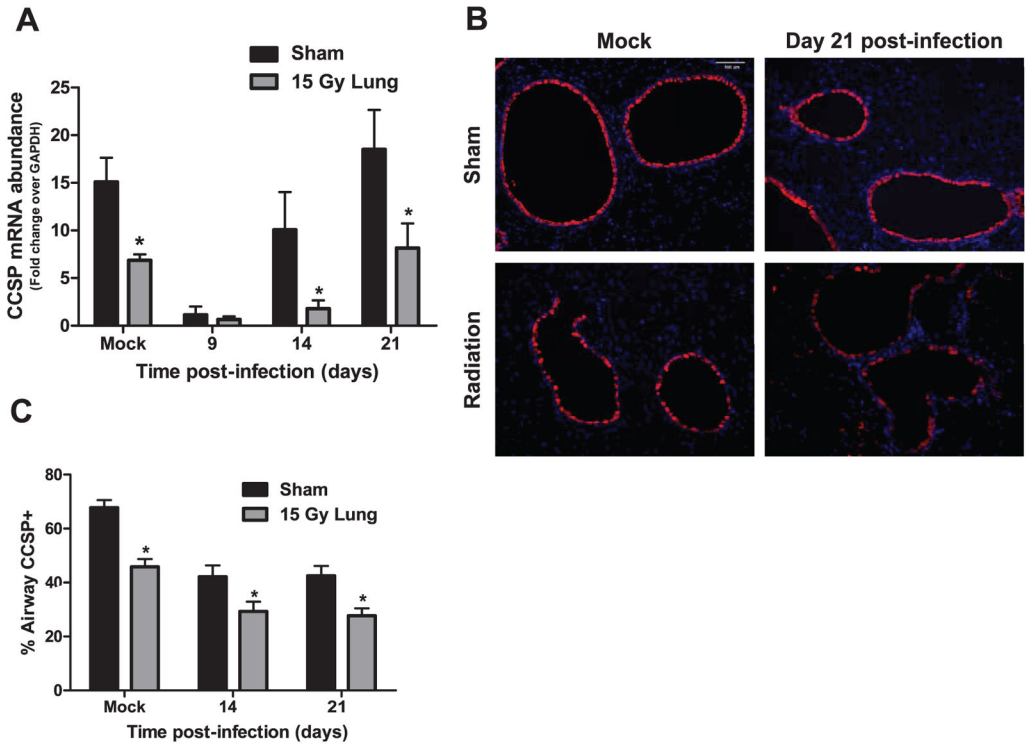

FIG. 4.

Clara cell secretory protein (CCSP) mRNA and CCSP protein expression in airway epithelial cells after infection in sham and irradiated mice. At 10 weeks post-irradiation, sham and 15 Gy whole-lung irradiated mice were infected with 120 HAU influenza A virus. CCSP was used as a marker for airway epithelial Clara cells. Panel A: CCSP mRNA abundance in the lungs at 9, 14 and 21 days post-infection. Abundance is expressed as fold change over GAPDH internal control. (Two-way ANOVA with Fisher's post-test, $*P < 0.05$ versus sham-infected, $n = 3–6$ per group.) Panel B: Representative images (10×) of CCSP-expressing cells (red) in mock-infected animals and at day 21 post-infection. Panel C: Percentage of airway staining positive for CCSP in mock-infected or virus-infected sham and irradiated groups. Two-way ANOVA with Fisher's post-test, $*P < 0.05$ versus sham-infected, $n = 3–6$ per group.

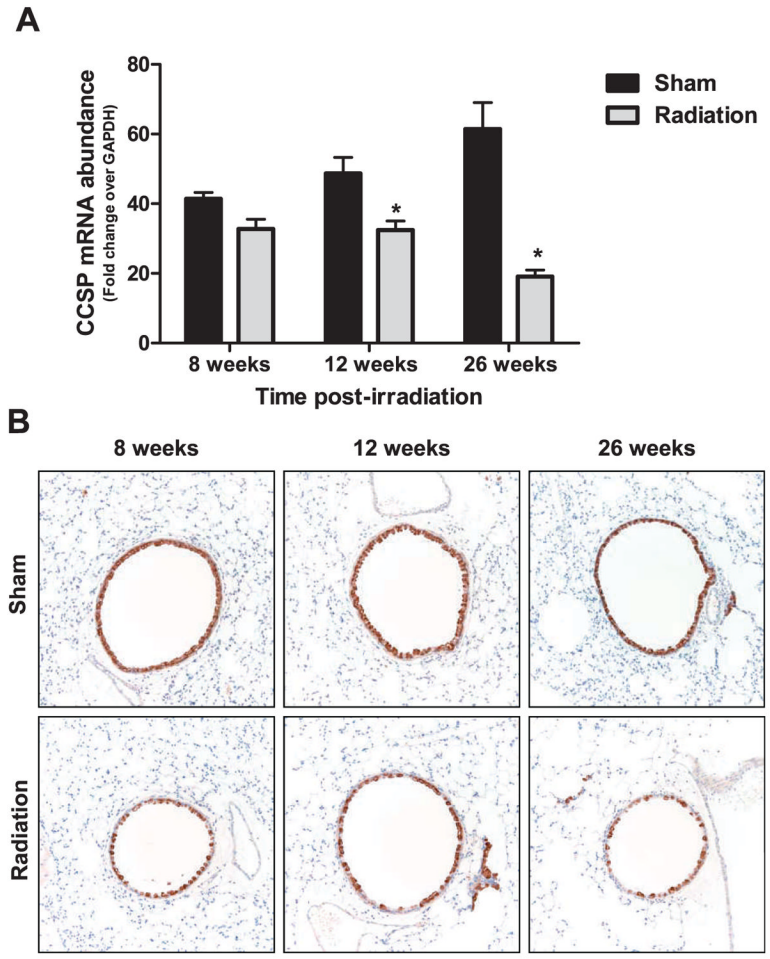

FIG. 5.

CCSP mRNA and CCSP protein expression in airway epithelial cells after irradiation alone. Panel A: CCSP mRNA abundance in the lungs at 8, 12 and 26 weeks after 15 Gy whole-lung irradiation. Abundance is expressed as fold change over GAPDH internal control. Data are expressed as mean ± SEM. Data were analyzed by two-way ANOVA with Fisher's post-test (* $P < 0.05$ versus sham-infected, $n = 10$ per group). Panel B: Representative images (20×) of CCSP-expressing cells in the airways (brown) of sham and irradiated animals at each time point.

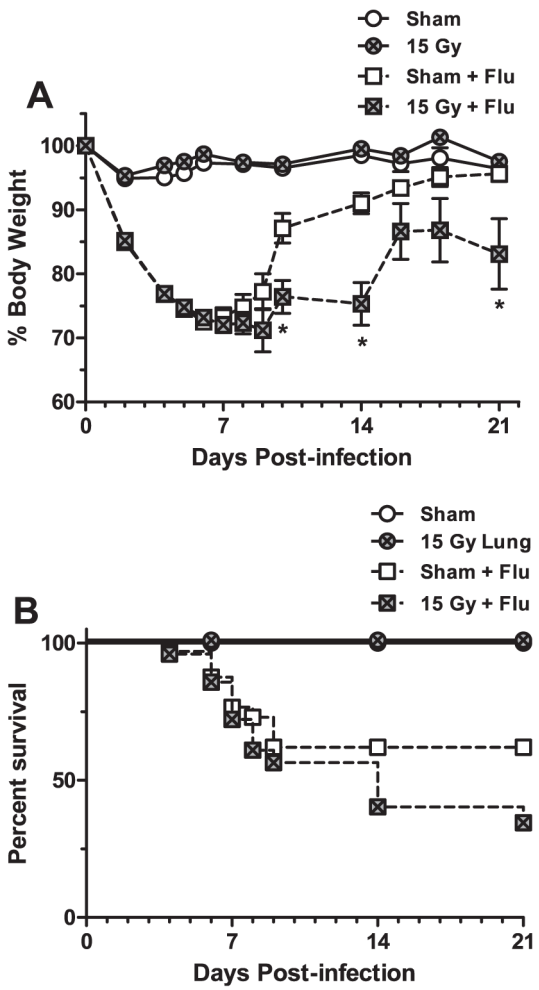

FIG. 6.

The pulmonary immune response after influenza A virus infection in sham and 15 Gy whole-lung irradiated CCSP$^{-/-}$ mice. CCSP$^{-/-}$ mice were infected with 120 HAU influenza A virus at 10 weeks post-irradiation. Panel A: Body weight changes over time. Changes in body weight were used as an indicator of morbidity after infection and are expressed as a percentage of body weight at the time of infection. (Two-way ANOVA with Fisher's post-test, $*P < 0.05$ versus sham-infected, $n = 30$ for virus-infected groups, $n = 7$ for mock-infected groups.) Panel B: Kaplan-Meier survival curves presenting mean survival of each group throughout 21 days post-infection. Curves were analyzed using the log rank test. The difference in mortality between the sham-infected and irradiated-infected groups was not significant ($P = 0.1547$).

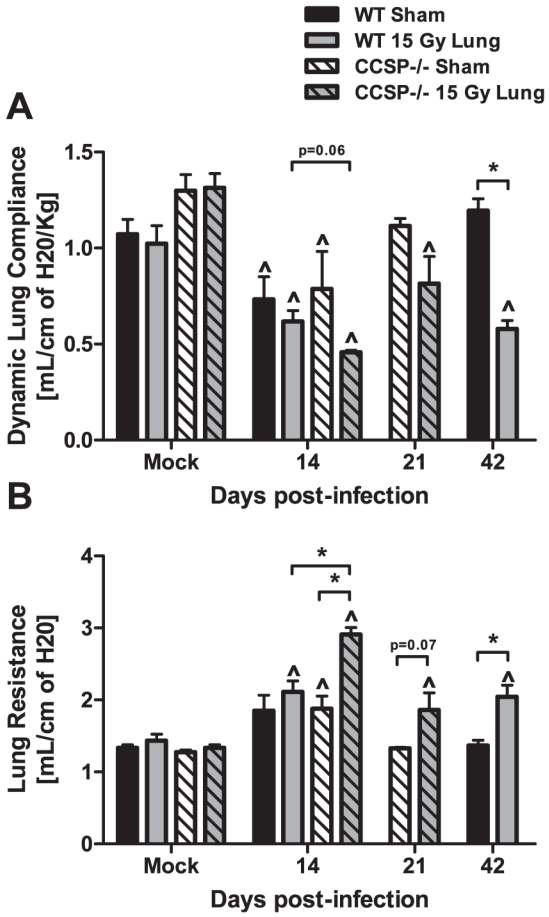

FIG. 7.

Comparison of pulmonary function after infection in irradiated wild-type and CCSP$^{-/-}$ mice. Pulmonary function was assessed in sham and irradiated CCSP$^{-/-}$ mice at days 14 and 21 post-infection using whole body plethysmography. Pulmonary function data from wild-type mice, presented in Fig. 2, was re-graphed for comparison to CCSP$^{-/-}$ mice. Panel A: Dynamic lung compliance and (panel B) lung resistance at days 14 and 21 post-infection (Two-way ANOVA with Fisher's post-test, $^{\wedge}P < 0.05$ versus mock-infected control, $*P < 0.05$ versus infected sham group; $n = 4$ per group).

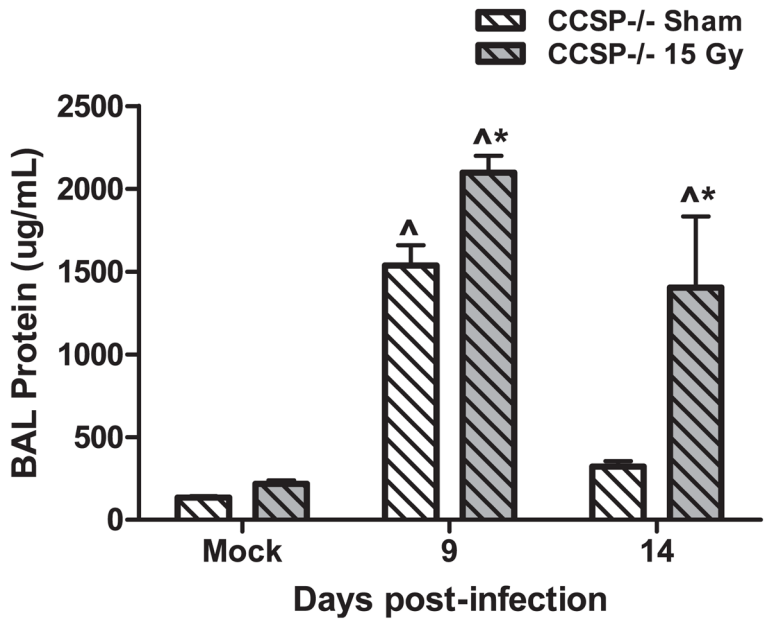

FIG. 8.

Total protein in the bronchoalveolar lavage fluid in irradiated $CCSP^{-/-}$ animals infected with influenza A virus. $CCSP^{-/-}$ mice were infected with influenza A virus, 10 weeks post-sham or 15 Gy whole-lung irradiation. Total protein in the BAL fluid in mock-infected animals and at days 9 and 14 post-infection was measured using the Coomassie Blue assay. (Two-way ANOVA with Fisher's post-test, $*P < 0.05$ versus infected sham group; $n = 4–6$ per group.)

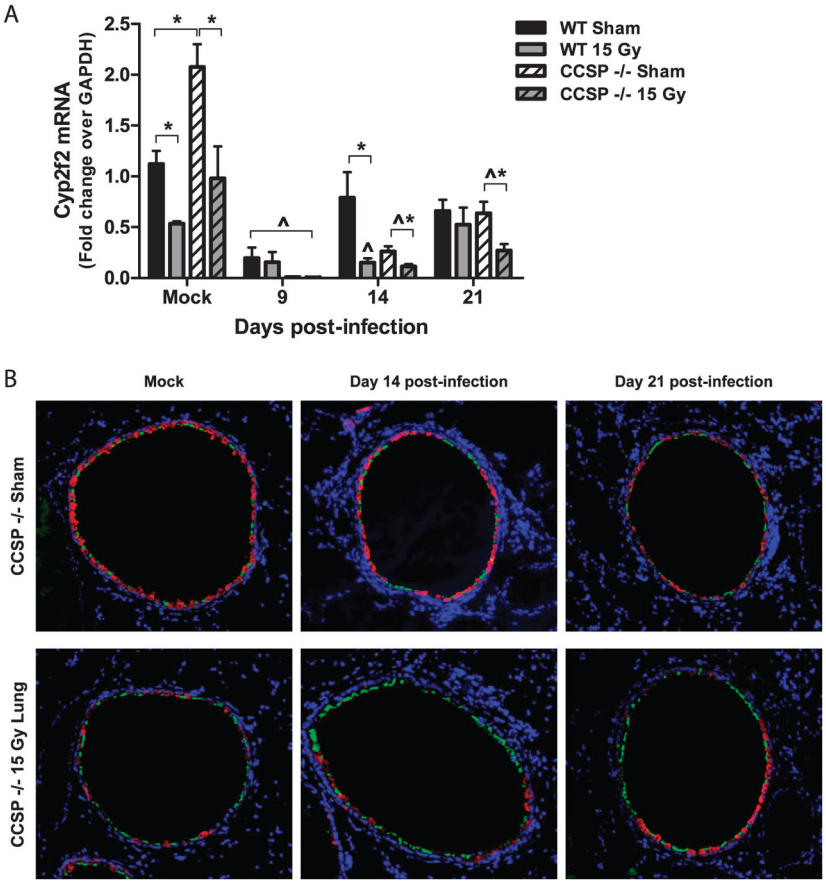

FIG. 9.

Cyp2f2 mRNA and immunofluorescence after irradiation and infection. Cyp2f2 was used as a Clara cell marker in CCSP$^{-/-}$ mice. Panel A: Cyp2f2 mRNA abundance was measured in the lungs on days 9, 14 and 21 post-infection in sham and irradiated CCSP$^{-/-}$ and wild-type mice. (Two-way ANOVA with Fisher's post-test, $*P < 0.05$ versus infected sham group; n =4–6 per group.) Panel B: Immunofluorescence for Cyp2f2 (red) and acetylated alpha-tubulin (green), a ciliated airway epithelial cell marker, in sham and irradiated CCSP$^{-/-}$ mice after mock or influenza A virus infection. Images (10×) are representative of 4 mice per group.